Lateral transport of Smoothened from the plasma membrane to the membrane of the cilium

Ljiljana Milenkovic,[1] Matthew P. Scott,[1] and Rajat Rohatgi[2]

Howard Hughes Medical Institute,[1] Department of Developmental Biology,[1] Department of Genetics,[1] Department of Bioengineering,[1] Department of Medicine,[2] and Department of Biochemistry,[2] Stanford University School of Medicine, Stanford, CA 94305

The function of primary cilia depends critically on the localization of specific proteins in the ciliary membrane. A major challenge in the field is to understand protein trafficking to cilia. The Hedgehog (Hh) pathway protein Smoothened (Smo), a 7-pass transmembrane protein, moves to cilia when a ligand is received. Using microscopy-based pulse-chase analysis, we find that Smo moves through a lateral transport pathway from the plasma membrane to the ciliary membrane. Lateral movement, either via diffusion or active transport, is quite distinct from currently studied pathways of ciliary protein transport in mammals, which emphasize directed trafficking of Golgi-derived vesicles to the base of the cilium. We anticipate that this alternative route will be used by other signaling proteins that function at cilia. The path taken by Smo may allow novel strategies for modulation of Hh signaling in cancer and regeneration.

Introduction

Primary cilia, solitary projections found on the surface of most cells in our bodies, are complex organelles that detect and interpret a variety of extracellular signals (Gerdes et al., 2009). Work in several systems has suggested that the dynamic movement of receptors and other proteins into and out of cilia regulates the activity of signaling complexes that ultimately trigger responses in the cell (Corbit et al., 2005; Haycraft et al., 2005; Wang et al., 2006; Rohatgi et al., 2007; Kovacs et al., 2008). Thus, a central challenge in the field is to understand how transmembrane proteins are targeted to cilia and how this targeting can be regulated by signals. The trafficking of proteins to the primary cilium, a tiny structure <5 µm long and <1 µm wide, presents a formidable challenge: in a cultured fibroblasts, the base of the cilium (the target zone for proteins sent to cilia) has a surface area that is >2,000-fold smaller than the rest of the plasma membrane.

Current models for membrane protein trafficking to primary cilia highlight the importance of directed vesicular trafficking from the Golgi apparatus along microtubule tracks to the base of the cilium (Fig. 1; Rosenbaum and Witman, 2002; Pazour and Bloodgood, 2008). This model is supported both by the physical proximity of the Golgi to the basal body (Sorokin, 1962) and by functional studies showing that the transport of rhodopsin to specialized primary cilia, the outer segments of photoreceptors, is blocked by disruption of Golgi membranes with the drug Brefeldin A (Deretic and Papermaster, 1991; Moritz et al., 2001). Recent efforts have focused on discovering the protein machinery that sorts proteins at the Golgi into vesicles that are directed to the base of the primary cilium (Follit et al., 2006; Omori et al., 2008).

Two additional trafficking routes can be envisioned for transmembrane proteins movement to primary cilia (Fig. 1). First, proteins could be transported laterally from the plasma membrane into the membrane of the cilium by breaching the diffusion barrier postulated to exist at the base of the cilium (the "lateral transport pathway"; Musgrave et al., 1986; Hunnicutt et al., 1990). Second, proteins located at the plasma membrane could move into endocytic vesicles that traffic to the base of the cilium (the "recycling pathway"). These pathways would likely be regulated by distinct sets of proteins.

To dissect these three trafficking routes to primary cilia, we used novel antibody and small-molecule affinity probes (Fig. 2 A), in combination with pulse-chase analysis of protein

L. Milenkovic and R. Rohatgi contributed equally to this paper.

Correspondence to Rajat Rohatgi: rrohatgi@stanford.edu; and Matthew P. Scott: mscott@stanford.edu

Abbreviations used in this paper: CBG, C8 propanoic acid benzylguanine; DIP, dynamin inhibitory peptide; Fsk, Forskolin; Hh, Hedgehog; Ptc1, Patched 1; SAG, Smo agonist; Smo, Smoothened; Shh, Sonic hedgehog.

The Rockefeller University Press $30.00
J. Cell Biol. Vol. 187 No. 3 365–374
www.jcb.org/cgi/doi/10.1083/jcb.200907126

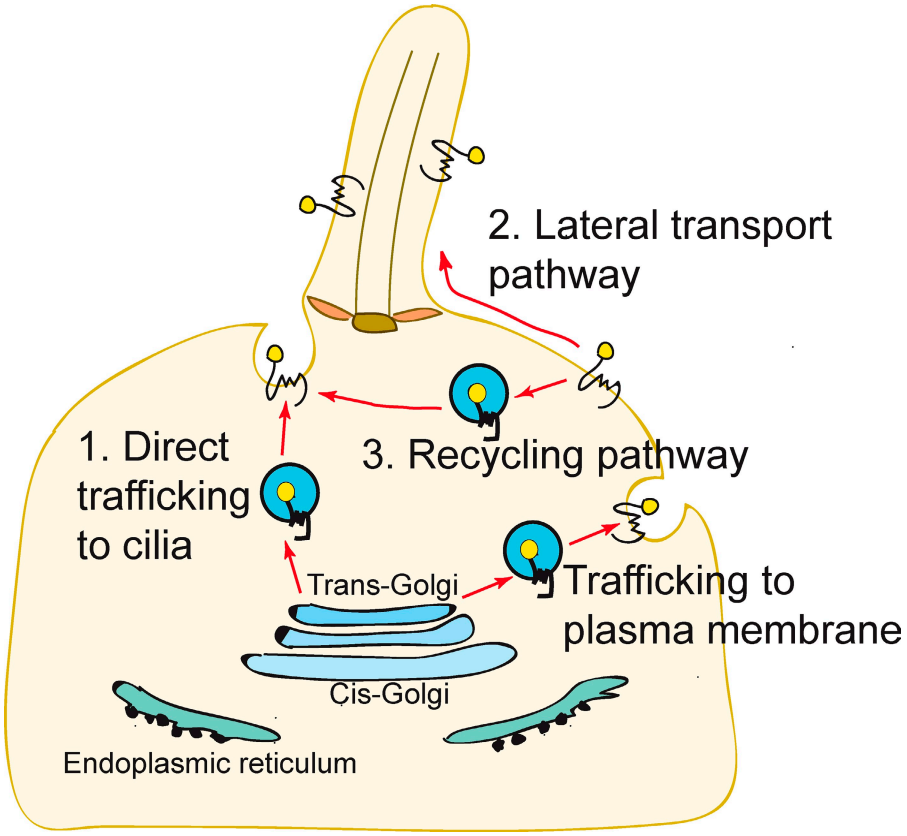

Figure 1. **Three models for Hh-induced Smo transport to the primary cilium.** (1) Direct trafficking from the Golgi to the base of the cilium. (2) Transport to the cell surface followed by lateral transport into the cilium. (3) Surface localization followed by internalization into a recycling pathway.

localization by fluorescence microscopy, to monitor the movement of the transmembrane protein Smoothened (Smo) to primary cilia. Smo, which is encoded by a human proto-oncogene, is a component of the Hedgehog (Hh) signal transduction pathway. Hh signaling is a cilium-associated pathway that plays fundamental roles in development, stem cell function, and carcinogenesis. The binding of the ligand Sonic Hedgehog (Shh) to its receptor Patched 1 (Ptc1) triggers the accumulation of Smo within the ciliary membrane and the activation of signaling (Corbit et al., 2005; Rohatgi et al., 2007). Drugs targeting Smo are being tested in human cancer patients and some of these compounds function by blocking Smo transport to cilia (Rohatgi et al., 2009; Scales and de Sauvage, 2009). In addition to shedding light on the problem of ciliary protein trafficking, an understanding of the molecular mechanisms underlying Smo accumulation in cilia will shed light into how this potentially oncogenic protein is activated.

Results and discussion

Smo is present on the cell surface and translocates to primary cilia after Shh stimulation

The recycling and lateral transport pathways (Fig. 1) require that Smo should be present on the plasma membrane of cells, which has been difficult to detect by simple fluorescence (Rohatgi et al., 2007). Using non–cell-permeable biotinylation, endogenous Smo could be readily detected on the surface of NIH3T3 cells (Fig. 2 B) before and after Shh addition. This assay cannot distinguish Smo on the plasma membrane from Smo on the ciliary membrane, so the location of Smo was also determined by microscopy. We reasoned that Smo on the cell surface would be labeled by an antibody against an epitope on the N-terminal region of the protein (Fig. 2 A). When *smo*−/− cells producing Smo tagged at its N terminus with YFP (YFP-Smo cells; Rohatgi et al., 2009) were exposed to an anti-YFP antibody, surface-exposed Smo could be readily detected before and after Shh addition (Fig. 2 C). The polyclonal anti-YFP antibody cross-linked surface YFP-Smo into aggregates visible over the entire plasma membrane, without any evidence for enrichment in a particular plasma membrane domain. YFP-Smo was detected at cilia only after Shh addition (Fig. 2 C, right). In control experiments, anti-YFP did not label *smo*−/− cells producing Smo fused to a different tag (Fig. S1 A). An antibody directed against an intracellular part of Smo (anti-SmoC; Rohatgi et al., 2007) did not label intact cells (Fig. S1 B). Thus, we conclude that Smo is present on the plasma membrane of both Shh-treated and untreated cells, which is consistent with the lateral transport or recycling models for transport.

If surface Smo undergoes transport into cilia, the aggregation of YFP-Smo by the anti-YFP antibody could block its movement to cilia, which is analogous to blocking the lateral diffusion of neurotransmitter receptors by antibody cross-linking on the surface of neurons (Ashby et al., 2006). Surface cross-linking should have little effect if delivery of Smo to the cilium involves exocytosis from internal pools upon addition of Shh. Consistent with the first possibility, treatment of cells with anti-YFP during the period of Shh exposure largely prevented transport of YFP-Smo to cilia (Fig. 2 D).

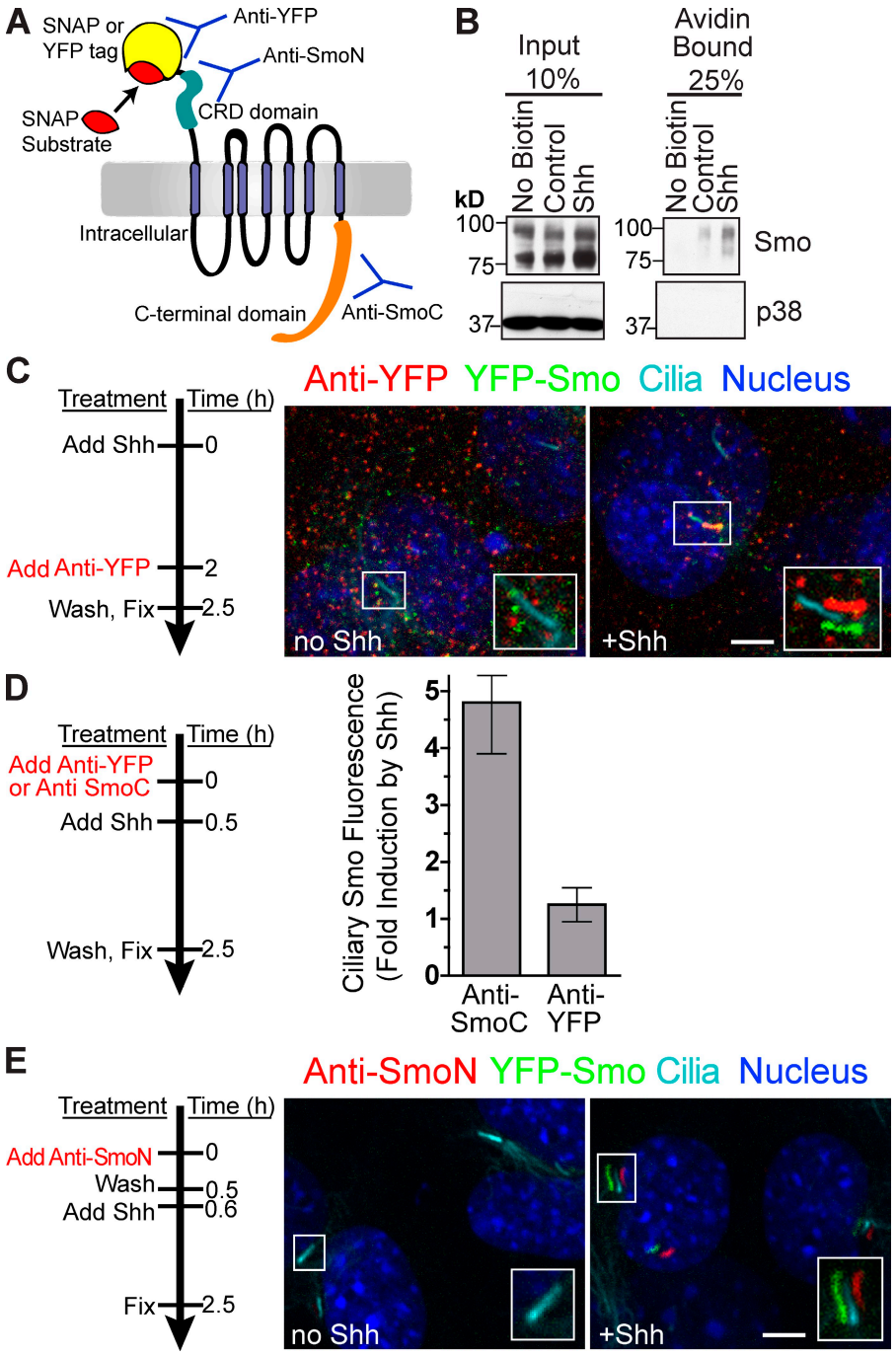

Figure 2. **Smo present on the cell surface translocates to the primary cilium after Shh stimulation.** (A) Extracellular domains of Smo are recognized by anti-YFP (YFP tag), anti-SmoN (cysteine-rich domain), or the SNAP substrate (SNAP tag). An intracellular region of Smo is recognized by anti-SmoC. (B) Cell surface proteins were biotinylated, isolated on streptavidin beads, and examined for the presence of Smo or a control intracellular protein (p38) by immunoblotting. (C–E) Live YFP-Smo cells (Rohatgi et al., 2009) were exposed to anti-YFP (C and D) or anti-SmoN (E) according to the timeline shown to the left of each panel. (C) Insets (enlarged views of the boxed regions) show cilia visualized as shifted overlays of the color channels. (D) Intensity of Smo fluorescence at cilia, shown as fold increase, after treatment with Shh in cells pretreated with anti-YFP or anti-SmoC (control). Data indicate mean ± SEM. (E) Shh was added after cells were treated with anti-SmoN. Both the main panels and insets (enlarged views of the boxed regions) showing cilia are shifted overlays. Bars, 5 µm.

Because anti-YFP induced the aggregation of YFP-Smo, it could not be used to monitor the movement of surface Smo to the cilium. We generated an antibody (anti-SmoN) that recognized the N-terminal cysteine-rich domain of Smo and, importantly, did not cross-link Smo into aggregates (Figs. 2 E and S1 C). YFP-Smo cells were surface-labeled with anti-SmoN and extensively washed to remove free antibody. Before addition of Shh, nonaggregated YFP-Smo labeled with anti-SmoN was below the limit of detection, likely because it was dispersed over the entire plasma membrane. In contrast, after the cells were treated with Shh, YFP-Smo labeled with anti-SmoN was seen localized in primary cilia (Fig. 2 E). The most parsimonious explanation for this result is that Shh causes Smo dispersed over the cell surface to concentrate in cilia, a result that is consistent with lateral transport or recycling models but not with directed vesicular transport. Controls excluded the possibility that incompletely washed anti-SmoN in the culture medium labeled YFP-Smo after its movement to cilia (Fig. S1 D).

Surface Smo enters cilia before intracellular Smo in response to Shh

Antibodies can alter the trafficking behavior of proteins, so we used a completely independent method to label Smo and follow its transport. Smo was tagged at its N terminus with the SNAP tag protein, a modified version of the enzyme O^6-alkylguanine-DNA-alkyltransferase, which can be rapidly and covalently

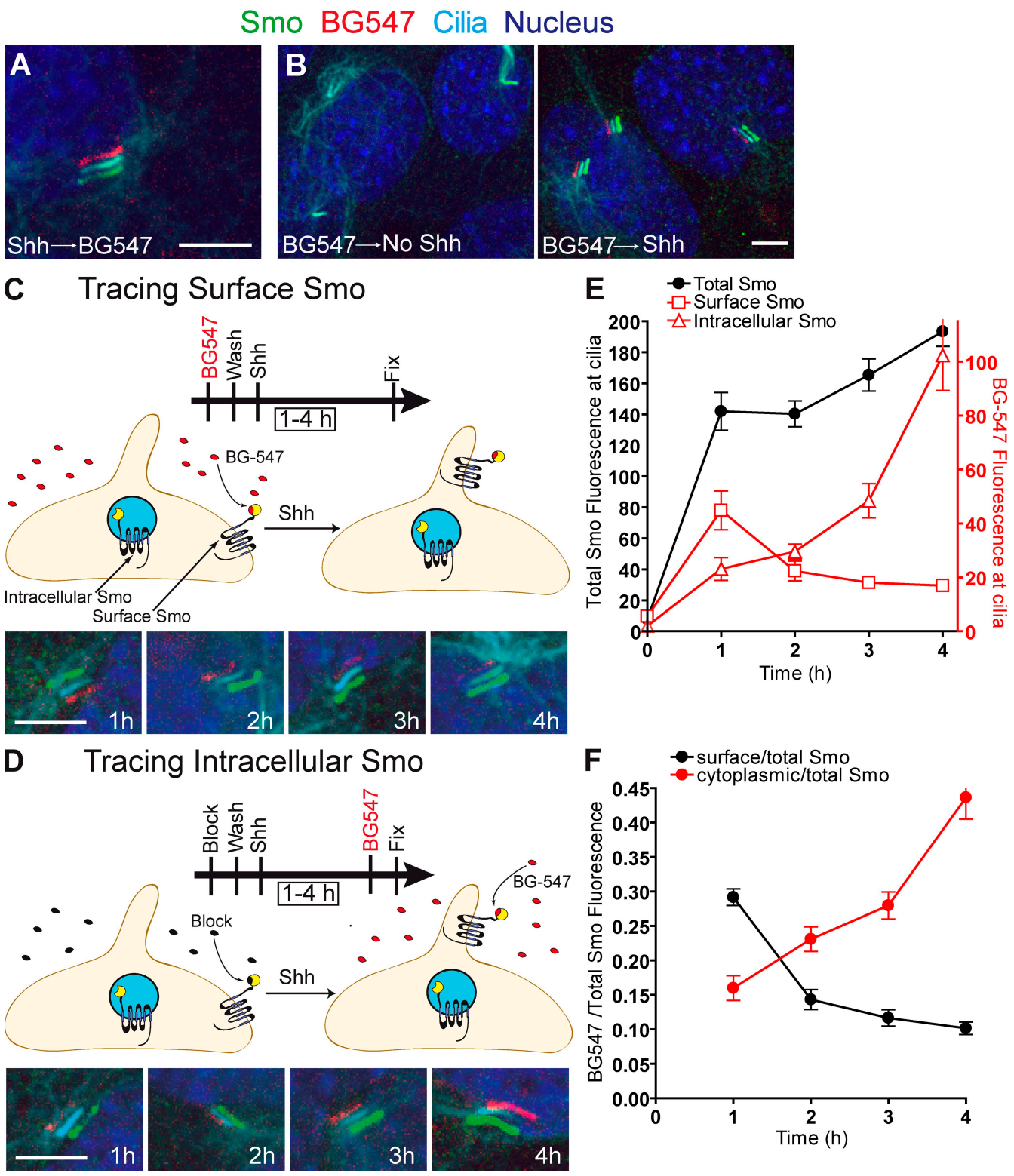

Figure 3. **Pulse-chase labeling: surface-derived Smo enters cilia before intracellular Smo in response to Shh.** All parts of the figure use cells expressing SNAP-tagged Smo. (A) Cells pretreated with Shh were labeled with the non–cell-permeable SNAP substrate BG-547. Shifted overlay shows that the BG-547 signal is coincident with cilia and the total SNAP-Smo protein detected with anti-SmoC. (B) Cells prelabeled with BG-547, washed, then treated with Shh show BG-547-labeled Smo localized at cilia. (C) To track Smo on cell surfaces, cells were treated as in B for the indicated periods of time. BG-547–labeled SNAP-Smo entered and then dissipated from the cilium. (D) To track intracellular Smo, SNAP-Smo on the cell surface was rendered invisible by treating cells with a non–cell-permeable block substrate (CBG block). After Shh treatment (times indicated), intracellular Smo that had translocated to the cilium was detected with BG-547 before fixation. Data from C and D were analyzed by plotting either the mean (±SEM) BG-547 and anti-SmoC fluorescence (E) or the mean BG-547/anti-SmoC fluorescence ratio (F) at various times after Shh treatment. Bars, 5 µm.

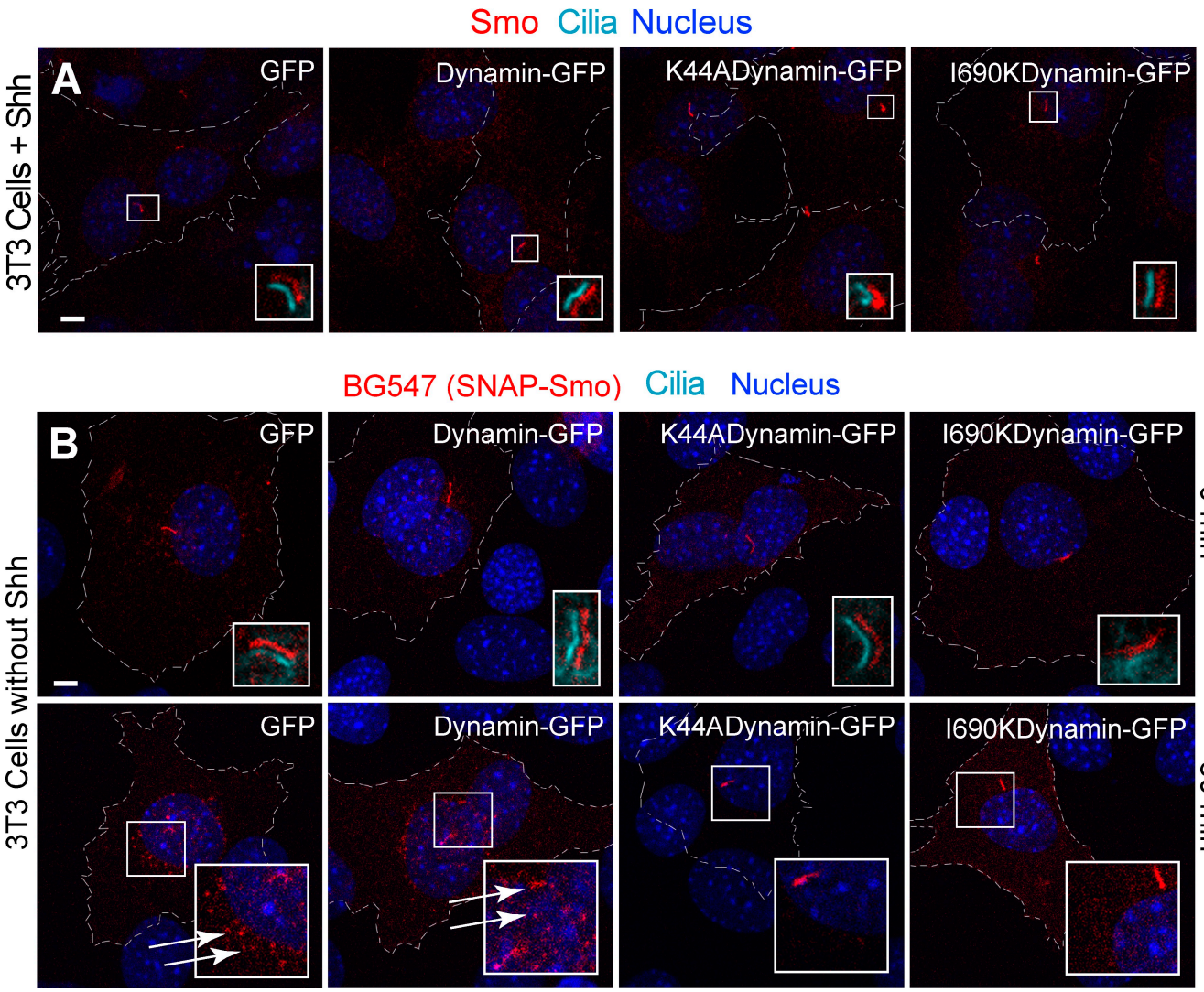

Figure 4. **Dynamin-dependent endocytosis is not required for Smo localization in the cilia.** (A) Dominant-negative dynamin mutants (K44A and I690K) did not block the translocation of endogenous Smo to cilia in Shh-treated (4 h) NIH3T3 cells. Transfected cells are outlined and were identified by GFP fluorescence (not shown for clarity), and insets show magnified views of cilia in the boxed regions (the ciliary marker acetylated tubulin is shown only in the insets as shifted overlays of two color channels). No Smo was detected at cilia in the absence of Shh in cells expressing any of the proteins (not depicted). (B) To establish that dominant-negative dynamin mutants can block the endocytosis of Smo, NIH3T3 cells were cotransfected with a SNAP-Smo gene and a gene encoding either wild-type dynamin or a dominant-negative dynamin. To follow the endocytosis of SNAP-Smo, cells were surface-labeled with non-permeable BG-547, washed to remove unreacted BG-547, and fixed immediately (top) or after incubation at 37° for 60 min to allow internalization (bottom). Cells transfected with wild-type dynamin but not dominant-negative dynamin show clear evidence for the internalization of BG-547-labeled Smo into a perinuclear compartment (indicated by arrows). The lack of perinuclear accumulation indicates that dominant-negative dynamin mutants (K44A and I690K) blocked the endocytosis of overexpressed Smo. Despite these differences in internalization, Smo is present in cilia under all conditions. Bars, 5 µm.

labeled with fluorescent small-molecule substrates (Fig. 2 A; Gautier et al., 2008). The SNAP-Smo protein retained functional activity because it restored Shh-induced target gene transcription to *smo*−/− cells and it translocated to cilia in response to Shh or Smo agonist (SAG; Fig. S2, A and B). SNAP-Smo present in the ciliary membrane of Shh-treated cells was readily labeled by BG-547, a non–cell-permeable substrate (Fig. 3 A). BG-547 labeling was specific: no labeling was seen in cilia lacking SNAP-Smo (not depicted), the BG-547 signal colocalized with anti-SmoC staining (Fig. 3 A), and quenching the SNAP tag with a nonfluorescent "blocking" substrate completely prevented BG-547 labeling (Fig. S2 C).

To determine whether the plasma membrane pool of Smo moves to cilia, surface SNAP-Smo was selectively labeled with BG-547 for 15 min and chased with a blocking substrate (Fig. 3 B). BG-547–labeled SNAP-Smo was detected at cilia after Shh treatment, so at least some of the Smo that entered cilia originated from the plasma membrane pool. BG-549, a more highly charged SNAP substrate, gave the same result (Fig. S2 D). Control experiments established that BG-547, BG-549, and the blocking substrates were not cell permeable (Fig. S2, E and F). This result again supports the lateral transport or recycling models for Smo transport to cilia because direct trafficking alone implies that no surface Smo moves to cilia.

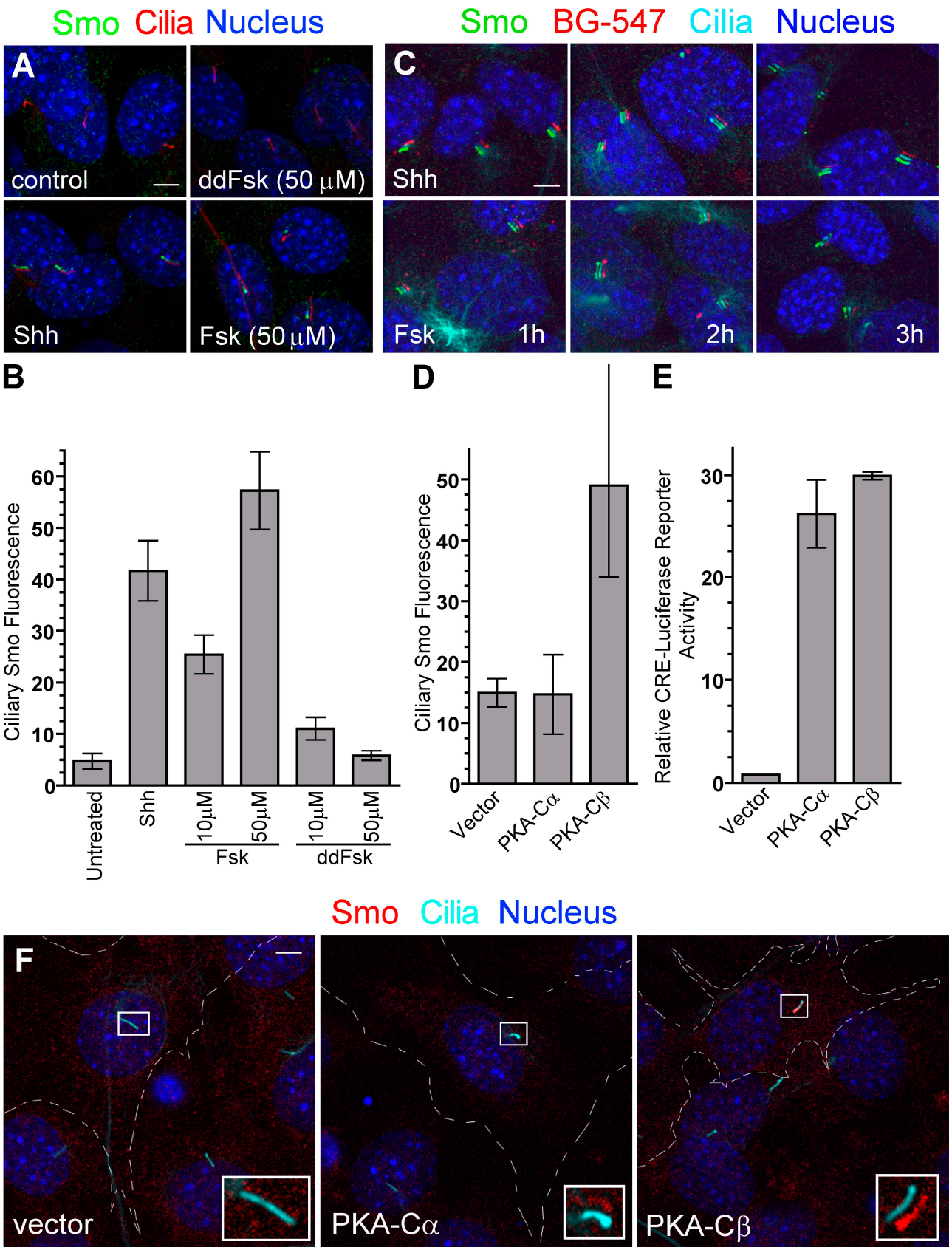

Figure 5. **The cAMP–PKA pathway promotes Smo entry into primary cilia.** (A and B) Smo is localized to primary cilia of NIH3T3 cells after treatment (4 h) with Shh or Fsk but not the inactive analogue dideoxy-Fsk (ddFsk). Representative images are shown in A, and mean (±SEM) ciliary Smo fluorescence is shown in B. (C) The labeling of surface SNAP-Smo (in SNAP-Smo cells) with non–cell-permeable BG-547 before treatment with Shh or Fsk shows that Fsk, like Shh, induces accumulation of BG-547-labeled Smo (surface Smo) in cilia by 1 h. The experiment timeline is as in Fig. 3 C. Images are shifted overlays

The lateral transport model posits that Smo follows a path from internal vesicles to the plasma membrane, and finally to the cilium (internal Smo → surface Smo → ciliary Smo). In comparison, the recycling model suggests that Smo moves from the surface into internal vesicles and then to the cilium (surface Smo → internal Smo → ciliary Smo). The critical difference is that after Shh addition, the initial source of Smo that enters primary cilia in the lateral transport model is from the plasma membrane; in the recycling model, it is from intracellular vesicles (Fig. 1). Pulse-chase analysis allowed us to establish the temporal order in which surface and intracellular Smo pools moved to cilia. To track surface Smo, SNAP-Smo cells were surface-labeled with BG-547 and exposed to Shh for various times (Fig. 3 C). To selectively track intracellular Smo, surface SNAP-Smo was reacted with a non–cell-permeable blocking substrate (Fig. 3 D), rendering this pool invisible. Cells were then treated with Shh for various periods and labeled with BG-547 immediately before fixation. BG-547 could label only SNAP-Smo molecules that had been intracellular and thus not accessible to the block. This strategy allowed us to use the same SNAP substrate to label surface and intracellular pools of Smo, thus avoiding possible artifacts caused by using different substrates. In both experiments, cells were also labeled with anti-SmoC to detect total Smo protein at cilia after fixation. Using quantitative microscopy, the BG-547 signal and the total Smo signal were measured for each individual cilium (Fig. 3, E and F). As expected, total Smo at cilia steadily increased after the addition of Shh (Rohatgi et al., 2007). Levels of surface-labeled SNAP-Smo peaked in cilia 1 h after Shh stimulation but then declined (Fig. 3, E and F), probably because the Smo protein at cilia was turning over. Smo protein has a half-life of about 2 h (Fig. S3 A). In contrast, intracellular SNAP-Smo reached cilia after a lag phase, which is consistent with delayed entry compared with the surface pool (Fig. 3, E and F). The delayed entry of intracellular Smo was confirmed in an independent experiment using a cell-permeable SNAP substrate to selectively label the intracellular pool before Shh stimulation (Fig. S3 B).

Collectively, the above results are consistent with Smo leaving the secretory pathway, moving to the plasma membrane, and undergoing lateral movement into the cilium after Shh addition. It is important to note that total Smo protein in the cell, and Smo protein localized in cilia, turned over quite rapidly, with a half-life on the order of 2 h (Fig. S3). Thus, even at early time points, e.g., 1 h after Shh addition, a fraction of ciliary Smo was replenished by new protein from the secretory pathway. The relatively rapid turnover of surface Smo might explain why a previous study did not detect movement of surface Smo to the cilium (Wang et al., 2009). In that study, localization of surface Smo in cilia was examined at a single time point, 2.5 h after stimulation with Shh, which was significantly later than the peak of newly arrived Smo at cilia revealed by our kinetic analysis. Based on our measurement of the Smo half-life using cycloheximide chase experiments (Fig. S3 A), much of the surface Smo protein will have turned over in 2.5 h, perhaps reducing its levels to below those required for detection.

Dynamin-dependent endocytosis is not required for Smo localization in the cilia

To further distinguish recycling and lateral transport pathways, we tested whether inhibition of endocytosis affects Smo entry into cilia. Endocytosis should be required for the recycling pathway but not for lateral transport (Fig. 1). Overexpression of either of two well-characterized dominant-negative forms of dynamin (Song et al., 2004), the GTPase that drives scission of endocytic vesicles, did not block Shh-induced Smo transport to cilia, which supports the lateral transport model (Fig. 4 A). Control experiments demonstrated that the mutant dynamin proteins blocked endocytosis of the model cargo transferrin (Fig. S1 H) and blocked endocytosis of overexpressed Smo from the plasma membrane (Fig. 4 B). Interestingly, the mutant dynamin proteins had little effect on the localization of overexpressed Smo at primary cilia in the same cells in which internalization of surface Smo was effectively blocked (Fig. 4 B, bottom row), reaffirming that ciliary localization is not dependent on endocytosis. These results using dominant-negative dynamin mutant proteins were confirmed in independent experiments using a cell-permeable peptide that disrupts the interaction between dynamin and amphiphysin (Fig. S1, F and G).

The cAMP–PKA pathway promotes Smo entry into primary cilia

The lateral transport of proteins to the cilia has not been described in mammals, but a *Chlamydomonas reinhardtii* transmembrane protein, agglutinin, moves to flagella by lateral transport through a pathway stimulated by cAMP (Hunnicutt et al., 1990). Evidence for a positive role for cAMP and PKA in Smo regulation in *Drosophila* and mammals (Jia et al., 2004; Hallikas et al., 2006; Tiecke et al., 2007; Zhao et al., 2007; Wilson et al., 2009) has been described, so we tested cAMP and PKA effects on Smo localization. Treatment of cells with Forskolin (Fsk), which increases cAMP levels, induced translocation of Smo to primary cilia through a lateral transport pathway analogous to that regulated by Shh (Fig. 5, A–C). The effect of Fsk is probably mediated by PKA because overproduction of the catalytic subunit of PKA also induced Smo accumulation in cilia (Fig. 5, D and F). Of the two PKA isoforms tested, PKA-Cβ was more effective than PKA-Cα at inducing Smo movement to cilia. Both isoforms were equally effective in inducing the transcription of a cAMP response element–luciferase reporter gene (Fig. 5 E). Inhibition of PKA activity with two small-molecule inhibitors, H89 and KT5720, blocked Shh-induced activation of two target genes, *ptc1* and *gli1*, which is consistent with a positive role for PKA in Hh signal transduction (Fig. S1 I). The evolutionarily conserved

of the color channels. (D) The mean (±SEM) Smo fluorescence at cilia of transfected cells from the experiment shown in F. (E) The same PKA-Cα and PKA-Cβ constructs used in C were tested for their abilities to induce a cAMP response element–linked luciferase reporter. (F) Cells transfected with genes encoding either the α or β catalytic subunit of PKA were stained to show cilia and Smo. Broken lines demarcate transfected cells. Insets are magnified shifted overlays (indicated by the boxed regions) of two color channels. Bars, 5 µm.

ability of cAMP to regulate the movement of membrane proteins by lateral transport in *C. reinhardtii* and mammals suggests that this important second messenger may play a general role in regulating the transport of signaling proteins to primary cilia.

Our demonstration that Smo moves to cilia by lateral transport is unexpected, given current models for direct vesicular transport from the Golgi. The results focus attention on the diffusion barrier that separates the plasma membrane from the ciliary membrane, allowing the two contiguous membrane domains to maintain distinct compositions. The base of the cilium has long been postulated to function as a diffusion barrier (Sorokin, 1962; Vieira et al., 2006), but the molecular nature of this barrier and the molecular pathways that might allow proteins such as Smo to penetrate this barrier remain unknown. Smo might traverse this barrier and accumulate in cilia either via a diffusion-trap mechanism, similar to that used by neurotransmitter receptors to accumulate in dendritic spines (Ashby et al., 2006), or by an undiscovered active transport mechanism. The movement of Smo, including the methods developed here to monitor its lateral transport, should provide a facile system to study lateral transport to cilia.

Materials and methods

Constructs

Wild-type mouse Smo was tagged at the N terminus (with the insertion C terminal to the signal sequence) with YFP or the SNAP tag in the pCS2+ vector. For retroviral infections, SNAP-Smo and YFP-Smo were subcloned into pMSCV-pac. To produce retroviral supernatants, Bosc23 packaging cells were transfected using Fugene-6, supernatants containing viral particles were collected 48 h after the transfection, polybrene was added at 4 µg/ml, and supernatants were filtered through a 0.45-µm filter and used to infect fibroblasts (Pear et al., 1993; Bailey et al., 2002). The constructs for the catalytic subunits of PKA (both α and β; Uhler and McKnight, 1987) were obtained from Addgene, and the cAMP response element–driven luciferase reporter (pGL4.29) was obtained from Promega. Constructs encoding GFP-tagged wild-type dynamin or the two dominant-negative dynamin proteins were provided by S. Schmid (The Scripps Research Institute, La Jolla, CA).

Small molecules and recombinant proteins

SAG, Fsk, H-89, and KT5720 were obtained from Enzo Life Sciences, Inc.; dynamin inhibitory peptide (DIP) and a control scrambled peptide (CIP) were obtained from Tocris Bioscience; dideoxy-Fsk was obtained from EMD; the SNAP substrates were obtained from Covalys and New England Biolabs, Inc.; and the puromycin and cycloheximide were obtained from Sigma-Aldrich. The 293 EcR Shh cells used to make Shh-conditioned media are available from American Type Culture Collection (ATCC; CRL-2782). They carry a stably integrated construct for full-length mouse Shh under an ecdysone-inducible promoter. The Shh produced by these cells is expected to be processed via an autocatalytic reaction, undergoing internal cleavage and lipidation. To produce conditioned media, cells were grown in high glucose Dulbecco's minimum essential medium, 0.05 mg/ml penicillin, 0.05 mg/ml streptomycin, 2 mM GlutaMAX, 1 mM sodium pyruvate, and 0.1 mM MEM nonessential amino acid supplement containing 10% FBS (Hyclone, defined grade; Thermo Fisher Scientific). At the time of induction with 1.5 µM muristerone A, cells were switched to media containing 2% FBS. Conditioned media was collected after ~72 h of induction, filtered through a 0.22-µM filter, and snap frozen in liquid nitrogen. Conditioned media was used at a dilution of 1:4 or 1:5 unless otherwise noted.

Cell culture

NIH3T3 cells were obtained from ATCC. The *smo−/−*:YFP-Smo cells (Rohatgi et al., 2009) and *smo−/−*:SNAP-Smo cell lines were generated by infection of *smo−/−* cells (Sinha and Chen, 2006) with a retrovirus carrying YFP-Smo or SNAP-Smo cloned into pMSCVpac, followed by selection in 2 µg/ml puromycin and isolation of single clones. The 293 EcR Shh cells used to make Shh conditioned media are available from ATCC (Taipale et al., 2000).

For assays of ciliary Smo accumulation, cells were grown to confluence in medium (high-glucose Dulbecco's minimum essential medium, 0.05 mg/ml penicillin, 0.05 mg/ml streptomycin, 2 mM GlutaMAX, 1 mM sodium pyruvate, and 0.1 mM MEM nonessential amino acid supplement) containing 10% FBS (Hyclone, defined grade), then switched to medium containing 0.5% FBS for 24 h. All cells were transfected using Fugene6 (Roche).

Antibodies

Polyclonal rabbit antisera against mouse Smo (anti-SmoC) were produced and purified as described previously (Rohatgi et al., 2007). The anti-SmoN polyclonal antibody was produced (Josman Laboratories) against amino acids 36–234 of the mouse Smo protein, and affinity-purified before use. The mouse anti-acetylated tubulin antibody was obtained from Sigma-Aldrich, the anti-SNAP antibody was obtained from Thermo Fisher Scientific, the rabbit anti-YFP antibody was obtained from Abcam (ab290), and the goat anti–rabbit or goat anti–mouse secondary antibodies coupled to Alexa Fluor 594, Alexa Fluor 488, or Alexa Fluor 647 were obtained from Invitrogen.

Immunofluorescence and microscopy

Cultured cells were fixed with 4% PFA in PBS for 10 min at 4°C and washed three times with PBS. Fixed cells were placed in blocking solution (PBS with 1% vol/vol normal goat serum and 0.1% vol/vol Triton X-100) for 30 min. Primary antibodies (1:1,000 for anti-Smo or anti-acetylated tubulin) were diluted in blocking solution and used to stain cells for 1 h at room temperature. After washing three times in PBS, Alexa Fluor–coupled secondary antibodies were added in blocking solution at 1:500 for 1 h at room temperature. DAPI was included in the final washes before the samples were mounted in Fluoromount G (SouthernBiotech) for microscopy. Microscopy was performed on an inverted laser scanning confocal microscope (DMIRE2; Leica). Images were taken with a 63× objective lens and 4× zoom (Leica). When possible, images were depicted with the color channels slightly shifted relative to each other ("shifted overlay") to more clearly show colocalization of different probes in the cilia. In all figures, the scale bar is 5 µm.

Antibody labeling experiments

In all panels, cilia and total Smo protein were detected with anti-acetylated tubulin or anti-SmoC, respectively, after cell permeabilization. For live cell antibody labeling, cells were incubated (30 min, 37°C) in media containing 0.5–1 µg/ml anti-SmoC, 1:1,000 anti-YFP, or 1–2 µg/ml anti-SmoN. After washing and fixation, the antibodies were detected with a secondary antibody before cell permeabilization. Cilia were labeled after a second washing and permeabilization step. For antibody-chase experiments, cells were washed three times with warm media after antibody feeding and then chased for an additional 2 h in the presence or absence of Shh.

SNAP labeling and pulse-chase

SNAP fluorescent substrates were used at 5 µM, non–cell-permeable C8 propanoic acid benzylguanine (CBG) block were used at 20 µM, and cell-permeable benzylguanine (BG) block were used at 10 or 20 µM. Live cells expressing SNAP-tagged proteins were stained for 15 min at 37°C. In control experiments to test the cell permeability of fluorescent substrates, the labeling period was extended to 30 or 60 min to make sure that substrates did not leak into the cell even in this prolonged period. For pulse-chase experiments, nonfluorescent blocking substrates were added during the chase period. For tracing surface Smo in pulse-chase experiments, cells were labeled with BG-547, washed, treated with Shh or other agonists, and fixed at different time points after induction. Two different approaches were taken to trace intracellular Smo. First, cell-surface Smo was blocked with CBG block (a non–cell-permeable molecule), and intracellular Smo was labeled with BG-505, a cell-permeable SNAP substrate. After washing off free BG-505, cells were exposed to an Hh agonist for varying periods of time before fixation. In an alternative approach, surface Smo was blocked with CBG block before cells were exposed to Shh. At different time points after Shh addition, cells were stained with BG-547 immediately before fixation to selectively reveal intracellular Smo that had moved to the cilium. The first approach detects only those Smo molecules that were present in the cell at the beginning of the experiment before Shh, whereas the second approach detects all Smo that is on the surface at the time of fixation, whether it existed at the beginning of the experiment or was newly delivered during the experiment. In all of the experiments, cells were stained after fixation and permeabilization with anti-SmoC to detect total Smo.

Surface biotinylation

Cells treated with Shh for 1 h were cooled to 4°C and biotinylated for 15 min with the cleavable cross-linker sulfo-NHS-S-S-biotin (Thermo Fisher Scientific). After quenching any remaining reagent, cells were

lysed, and biotinylated proteins were isolated on streptavidin-linked magnetic beads (Invitrogen). Proteins were eluted with sample buffer containing DTT (100 mM) and analyzed by immunoblotting.

Inhibition of endocytosis

Two different approaches were taken to block endocytosis: incubation of cells with a soluble, cell-permeable DIP (Marks and McMahon, 1998); or transfection of cells with GFP-tagged dominant-negative mutants of dynamin (K44A and I690K), previously shown to block endocytosis (Song et al., 2004). For experiments with DIP, NIH3T3 cells were incubated with DIP or a scrambled control peptide for 30 min before the addition of Shh or SAG for 2 h. Transferrin uptake was used to assess the efficiency of DIP and dynamin mutants in blocking endocytosis.

Transferrin uptake

Alexa Fluor 594–conjugated transferrin (50 µM) from Invitrogen was added to cells in serum-free media and allowed to bind at room temperature for 2 min. After the binding, cells were washed with media and incubated for 15 min at 37°C to allow internalization. Cells were rapidly cooled by adding chilled media to stop further endocytosis, acid-washed (0.1 M glycine, pH 2.5, and 150 mM NaCl) to strip off surface-bound (but not internalized) transferrin, and fixed for analysis.

Image and data analysis

All analysis was performed by importing images as TIFF files into ImageJ. For the quantitative analysis of Smo levels in primary cilia, all images used for comparisons within an experiment were taken with identical gain, offset, and laser power settings on the microscope and used for quantitation without any manipulation. A mask was constructed by manually outlining cilia in the image taken in the acetylated-tubulin channel. This mask was applied to the image taken in the Smo channel and the fluorescence at cilia measured. Local background correction was performed by moving the mask to measure fluorescence at a representative nearby region, and this value was subtracted from that of ciliary fluorescence. All points represent mean (±SEM) fluorescence from ∼10–30 individual cilia.

The data shown in Fig. 3 were quantified in two ways. Fig. 3 has two parallel but separate experiments, one in which surface Smo is followed and a second in which internal Smo is followed (Fig. 3, C and D). In both cases, the level of total Smo was measured by staining with anti-SmoC. The anti-SmoC staining data from both experiments (Fig. 3, C and D) were combined, and the mean total Smo at each time point was plotted. In the experiments following surface or internal Smo, BG-547 staining at each time point was averaged and plotted. For Fig. 3 F, instead of averaging the signals separately, the ratio of the BG-547 signal to the anti-SmoC signal (this is roughly proportional to the fraction of total Smo that is labeled with BG-547) for each cilium was individually calculated. These ratios were averaged for the two separate experiments at each time point, yielding the two curves.

Online supplemental material

Fig. S1 shows controls for Fig. 2 (A–E), 4 (F–G), and 5 (I). Fig. S2 shows characterization of SNAP-Smo cells and SNAP substrates. Fig. S3 show that Smo protein undergoes constant turnover. Online supplemental material is available at http://www.jcb.org/cgi/content/full/jcb.200907126/DC1.

We thank Arjun Raj for discussions of Smo diffusion, Sandra Schmid for *dynamin* constructs, and James Chen, Anthony Oro, and Suzanne Pfeffer for critical reading of the manuscript.

M.P. Scott is an investigator of the Howard Hughes Medical Institute. R. Rohatgi was supported by a National Cancer Institute Pathway to Independence award (5K99CA129174).

Submitted: 22 July 2009
Accepted: 30 September 2009

References

Ashby, M.C., S.R. Maier, A. Nishimune, and J.M. Henley. 2006. Lateral diffusion drives constitutive exchange of AMPA receptors at dendritic spines and is regulated by spine morphology. *J. Neurosci.* 26:7046–7055. doi:10.1523/JNEUROSCI.1235-06.2006

Bailey, E.C., L. Milenkovic, M.P. Scott, J.F. Collawn, and R.L. Johnson. 2002. Several PATCHED1 missense mutations display activity in patched1-deficient fibroblasts. *J. Biol. Chem.* 277:33632–33640. doi:10.1074/jbc.M202203200

Corbit, K.C., P. Aanstad, V. Singla, A.R. Norman, D.Y. Stainier, and J.F. Reiter. 2005. Vertebrate Smoothened functions at the primary cilium. *Nature.* 437:1018–1021. doi:10.1038/nature04117

Deretic, D., and D.S. Papermaster. 1991. Polarized sorting of rhodopsin on post-Golgi membranes in frog retinal photoreceptor cells. *J. Cell Biol.* 113:1281–1293. doi:10.1083/jcb.113.6.1281

Follit, J.A., R.A. Tuft, K.E. Fogarty, and G.J. Pazour. 2006. The intraflagellar transport protein IFT20 is associated with the Golgi complex and is required for cilia assembly. *Mol. Biol. Cell.* 17:3781–3792. doi:10.1091/mbc.E06-02-0133

Gautier, A., A. Juillerat, C. Heinis, I.R. Corrêa Jr., M. Kindermann, F. Beaufils, and K. Johnsson. 2008. An engineered protein tag for multiprotein labeling in living cells. *Chem. Biol.* 15:128–136. doi:10.1016/j.chembiol.2008.01.007

Gerdes, J.M., E.E. Davis, and N. Katsanis. 2009. The vertebrate primary cilium in development, homeostasis, and disease. *Cell.* 137:32–45. doi:10.1016/j.cell.2009.03.023

Hallikas, O., K. Palin, N. Sinjushina, R. Rautiainen, J. Partanen, E. Ukkonen, and J. Taipale. 2006. Genome-wide prediction of mammalian enhancers based on analysis of transcription-factor binding affinity. *Cell.* 124:47–59. doi:10.1016/j.cell.2005.10.042

Haycraft, C.J., B. Banizs, Y. Aydin-Son, Q. Zhang, E.J. Michaud, and B.K. Yoder. 2005. Gli2 and Gli3 localize to cilia and require the intraflagellar transport protein polaris for processing and function. *PLoS Genet.* 1:e53. doi:10.1371/journal.pgen.0010053

Hunnicutt, G.R., M.G. Kosfiszer, and W.J. Snell. 1990. Cell body and flagellar agglutinins in *Chlamydomonas reinhardtii*: the cell body plasma membrane is a reservoir for agglutinins whose migration to the flagella is regulated by a functional barrier. *J. Cell Biol.* 111:1605–1616. doi:10.1083/jcb.111.4.1605

Jia, J., C. Tong, B. Wang, L. Luo, and J. Jiang. 2004. Hedgehog signalling activity of Smoothened requires phosphorylation by protein kinase A and casein kinase I. *Nature.* 432:1045–1050. doi:10.1038/nature03179

Kovacs, J.J., E.J. Whalen, R. Liu, K. Xiao, J. Kim, M. Chen, J. Wang, W. Chen, and R.J. Lefkowitz. 2008. Beta-arrestin-mediated localization of smoothened to the primary cilium. *Science.* 320:1777–1781. doi:10.1126/science.1157983

Marks, B., and H.T. McMahon. 1998. Calcium triggers calcineurin-dependent synaptic vesicle recycling in mammalian nerve terminals. *Curr. Biol.* 8:740–749. doi:10.1016/S0960-9822(98)70297-0

Moritz, O.L., B.M. Tam, L.L. Hurd, J. Peränen, D. Deretic, and D.S. Papermaster. 2001. Mutant rab8 Impairs docking and fusion of rhodopsin-bearing post-Golgi membranes and causes cell death of transgenic *Xenopus* rods. *Mol. Biol. Cell.* 12:2341–2351.

Musgrave, A., P. de Wildt, I. van Etten, H. Pijst, C. Scholma, R. Kooyman, W. Homan, and H. van den Ende. 1986. Evidence for a functional membrane barrier in the transition zone between the flagellum and the cell body of *Chlamydomonas eugametos* gametes. *Planta.* 167:544–553. doi:10.1007/BF00391231

Omori, Y., C. Zhao, A. Saras, S. Mukhopadhyay, W. Kim, T. Furukawa, P. Sengupta, A. Veraksa, and J. Malicki. 2008. Elipsa is an early determinant of ciliogenesis that links the IFT particle to membrane-associated small GTPase Rab8. *Nat. Cell Biol.* 10:437–444. doi:10.1038/ncb1706

Pazour, G.J., and R.A. Bloodgood. 2008. Targeting proteins to the ciliary membrane. *Curr. Top. Dev. Biol.* 85:115–149. doi:10.1016/S0070-2153(08)00805-3

Pear, W.S., G.P. Nolan, M.L. Scott, and D. Baltimore. 1993. Production of high-titer helper-free retroviruses by transient transfection. *Proc. Natl. Acad. Sci. USA.* 90:8392–8396. doi:10.1073/pnas.90.18.8392

Rohatgi, R., L. Milenkovic, and M.P. Scott. 2007. Patched1 regulates hedgehog signaling at the primary cilium. *Science.* 317:372–376. doi:10.1126/science.1139740

Rohatgi, R., L. Milenkovic, R.B. Corcoran, and M.P. Scott. 2009. Hedgehog signal transduction by Smoothened: pharmacologic evidence for a 2-step activation process. *Proc. Natl. Acad. Sci. USA.* 106:3196–3201. doi:10.1073/pnas.0813373106

Rosenbaum, J.L., and G.B. Witman. 2002. Intraflagellar transport. *Nat. Rev. Mol. Cell Biol.* 3:813–825. doi:10.1038/nrm952

Scales, S.J., and F.J. de Sauvage. 2009. Mechanisms of Hedgehog pathway activation in cancer and implications for therapy. *Trends Pharmacol. Sci.* 30:303–312. doi:10.1016/j.tips.2009.03.007

Sinha, S., and J.K. Chen. 2006. Purmorphamine activates the Hedgehog pathway by targeting Smoothened. *Nat. Chem. Biol.* 2:29–30. doi:10.1038/nchembio753

Song, B.D., D. Yarar, and S.L. Schmid. 2004. An assembly-incompetent mutant establishes a requirement for dynamin self-assembly in clathrin-mediated endocytosis in vivo. *Mol. Biol. Cell.* 15:2243–2252. doi:10.1091/mbc.E04-01-0015

Sorokin, S. 1962. Centrioles and the formation of rudimentary cilia by fibroblasts and smooth muscle cells. *J. Cell Biol.* 15:363–377. doi:10.1083/jcb.15.2.363

Taipale, J., J.K. Chen, M.K. Cooper, B. Wang, R.K. Mann, L. Milenkovic, M.P. Scott, and P.A. Beachy. 2000. Effects of oncogenic mutations in Smoothened and Patched can be reversed by cyclopamine. *Nature.* 406:1005–1009. doi:10.1038/35023008

Tiecke, E., R. Turner, J.J. Sanz-Ezquerro, A. Warner, and C. Tickle. 2007. Manipulations of PKA in chick limb development reveal roles in digit patterning including a positive role in Sonic Hedgehog signaling. *Dev. Biol.* 305:312–324. doi:10.1016/j.ydbio.2007.02.017

Uhler, M.D., and G.S. McKnight. 1987. Expression of cDNAs for two isoforms of the catalytic subunit of cAMP-dependent protein kinase. *J. Biol. Chem.* 262:15202–15207.

Vieira, O.V., K. Gaus, P. Verkade, J. Fullekrug, W.L. Vaz, and K. Simons. 2006. FAPP2, cilium formation, and compartmentalization of the apical membrane in polarized Madin-Darby canine kidney (MDCK) cells. *Proc. Natl. Acad. Sci. USA.* 103:18556–18561. doi:10.1073/pnas.0608291103

Wang, Q., J. Pan, and W.J. Snell. 2006. Intraflagellar transport particles participate directly in cilium-generated signaling in *Chlamydomonas*. *Cell.* 125:549–562. doi:10.1016/j.cell.2006.02.044

Wang, Y., Z. Zhou, C.T. Walsh, and A.P. McMahon. 2009. Selective translocation of intracellular Smoothened to the primary cilium in response to Hedgehog pathway modulation. *Proc. Natl. Acad. Sci. USA.* 106:2623–2628. doi:10.1073/pnas.0812110106

Wilson, C.W., M.H. Chen, and P.T. Chuang. 2009. Smoothened adopts multiple active and inactive conformations capable of trafficking to the primary cilium. *PLoS One.* 4:e5182. doi:10.1371/journal.pone.0005182

Zhao, Y., C. Tong, and J. Jiang. 2007. Hedgehog regulates smoothened activity by inducing a conformational switch. *Nature.* 450:252–258. doi:10.1038/nature06225